APPLICATION NOTE

Quantum Parameter Extraction in QuantumPro

Methods for superconducting quantum circuits

KEYSIGHT

Table of Contents

Introduction 3

Full EM Analysis 4

Energy Participation Analysis 9

One Qubit One Readout Resonator Model 12

Four Qubits Four Resonators Model 15

Conclusion 18

References 19

Introduction

Superconducting qubits, the primary building blocks for superconducting quantum circuits, have been widely researched as a potential platform for complex quantum computation. Thanks to the GHz operational frequencies, superconducting qubits are manufactured in a macroscopic scale and have shown great promise especially in terms of scalability and robustness.

Superconducting qubits use a Josephson junction which is formed by two superconductors separated by a thin insulator. There is quantum tunneling across the insulator, a phenomenon known as the Josephson effect. The electrons bound within this junction display the characteristics of anharmonic oscillators with uneven quantized energy levels. Such anharmonicity allows for isolating two unique levels for quantum computing operations.

Superconducting qubits usually operate with readout resonators. Transmission line resonators, formed by open or short termination at both ends, are often used as readout resonators. When the resonances of the qubit and the resonator have a large frequency difference or a detuning, the qubits are said to be operating under a dispersive regime. The coupling between the superconducting qubits and the resonators effectively shifts the resonant frequency, a phenomenon that can help determine the characteristics of the quantum circuit.

In our recent application note, Designing for Superconducting Qubit Circuits, we detailed step-by-step guidelines to design basic superconducting circuits from scratch in PathWave Advanced Design System (ADS). We showed how to design a schematic/layout of a few qubits, simulate it, and create the GDS file for fabrication. Please review the application note for more information on the design and simulations of superconducting qubits.

Here, we discuss the methods QuantumPro utilizes to extract quantum parameters in detail. QuantumPro is designed to analyze quantum circuits that include Josephson junctions and readout resonators. The quantum parameters of superconducting quantum circuits can be calculated from a linear electromagnetic analysis by representing the qubits by their lumped inductances expected in the quantum regime at ultra-low signal excitation. QuantumPro extracts the quantum parameters using three methods; two are based on obtaining a frequency domain response [1-3] and one is based on finding an eigenmode solution [4, 5].

In QuantumPro, users may run two types of analyses: Full EM Analysis and Energy Participation Analysis. The former is a frequency domain analysis and supports the Finite Element Method (FEM) and the Method of Moment (MoM) while the latter supports the FEM eigenmode solver. The MoM approach is further split into Momentum RF and Momentum Microwave. Momentum RF takes a simpler approach based on quasi-static Green's functions. Therefore, it may not yield as high accuracy as Momentum Microwave at high frequencies, but it has lower computational complexity. FEM usually takes more computational resources due to the higher number of unknowns compared to the MoM solver.

In this application note, we discuss the EM simulation in QuantumPro, the math behind the determination of quantum parameters, and the comparison of quantum parameters obtained from different methods. We utilize the one-qubit-one-readout-resonator and the four-qubit-four-resonator examples to showcase the robustness of the methods.

Full EM Analysis

In this section, we discuss the frequency sweep method to extract the quantum parameters. This type of analysis is called the Full EM Analysis in QuantumPro. QuantumPro offers Momentum RF, Momentum Microwave, FEM, and the FEM eigenmode solvers, the first three of which are used in the Full EM Analysis. The difference between Momentum RF and Momentum Microwave is that the former resorts to a quasi-static approximation implying neglecting the high-frequency effects of the circuit. Therefore, it can obtain solutions within a shorter simulation timeframe. From here on, we use the terms Quasi-static (QS) Method for Momentum RF and Frequency Domain (FD) Method for Momentum Microwave and FEM.

Finding Qubit Anharmonicity

Utilizing Josephson junctions, superconducting qubits are renowned for showcasing notable nonlinearity, providing anharmonic oscillators that play a pivotal role as fundamental elements in quantum computing. While harmonic oscillators have quantized energy levels that are evenly spaced out, each energy level of an anharmonic oscillator has a slight frequency difference. Figure 1 depicts the quantized energy levels of such an anharmonic oscillator. For instance, if the transition frequency between the first two levels is denoted as ω_{01} and the transition frequency from the second level to the third as ω_{12}. There is a non-zero frequency difference between ω_{01} and ω_{12}. This difference allows for isolating one transition (e.g. $|0\rangle \rightarrow |1\rangle$) from all others to create the two-level system needed for qubits.

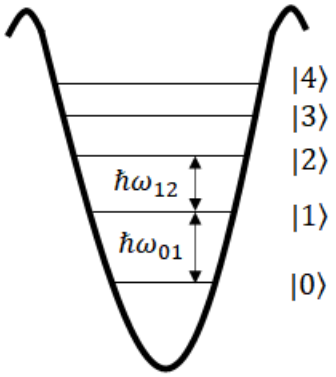

Figure 1. A quantized energy level diagram for an anharmonic oscillator. The energy spacing of each level differs from one another allowing for isolating a unique two-level system.

The first two transition energy levels of a superconducting qubit can be expressed as $\omega_{01} = \sqrt{8E_J E_C} - E_C$ and $\omega_{12} = \sqrt{8E_J E_C} - 2E_C$, respectively [1, 6, 7]. Here, E_J is the junction energy, and E_C is the charging energy of the qubit. The former relates to the qubit junction inductance while the latter relates to the qubit junction capacitance. The anharmonicity is then the difference between the two transition energies, $\alpha = \omega_{12} - \omega_{01}$ or namely, $\alpha = -E_C$.

The charging energy is defined as $E_c = e^2/2C$, where e is the electron charge and C is the total capacitance seen from the qubit port. In QuantumPro, users can explore this frequency-dependent capacitance from the scattering parameters. If the qubit is at Port 1, C11 would be the capacitance seen from the qubit. Figure 2 shows the solution obtained from the quasi-static (Momentum RF) and represents the capacitance of the qubit over the frequency range. Here, we are interested in the capacitance at the qubit resonant frequency, at around 6.12 GHz. The corresponding capacitance at this frequency for the qubit is 61.5 fF. The method to calculate the resonant frequency of the qubit is detailed in the following section.

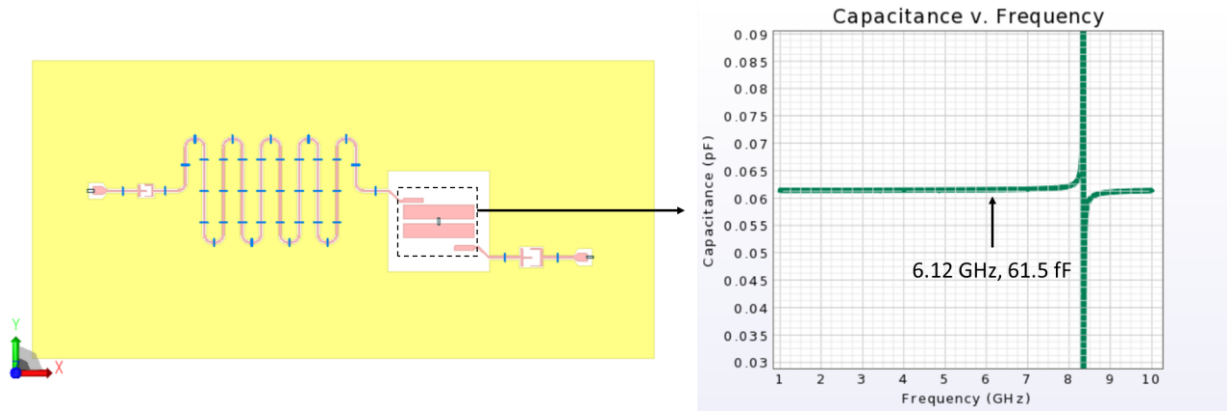

Figure 2. A one-qubit-one-readout example with the Momentum RF simulation. As shown in the plot on the right, the capacitance across the junction near the qubit resonant frequency (~ 6.12 GHz) is about 61.5 fF.

The quasi-static solution (Momentum RF) can be more quickly computed than the corresponding solutions using Momentum Microwave or FEM as it relies on a frequency-independent Green's function. This method produces fast results but to account for the high-frequency effects properly, Momentum Microwave is a more appropriate method in the context of Full EM Analysis.

Finding the Cross-Kerr

The Full EM Analysis allows for carrying out a frequency sweep using either FEM or Momentum RF/Microwave solvers. Based on the scattering parameters from the frequency sweep of the circuit, QuantumPro then calculates the resonant frequencies and the quantum parameters for qubits and resonators.

Due to the supercurrent arising from the Josephson effect, qubit junctions exhibit inductiveness. Therefore, as shown in Figure 3, the qubit can be modeled as a linear LC circuit. In QuantumPro, a port is defined across a qubit junction with a lumped inductor element (Q_InductorAbstract). For example, this model has six ports total, P1 and P2 being input/output ports and P1' for Q1, P2' for Q2, P3' for Q3, and P4' for Q4.

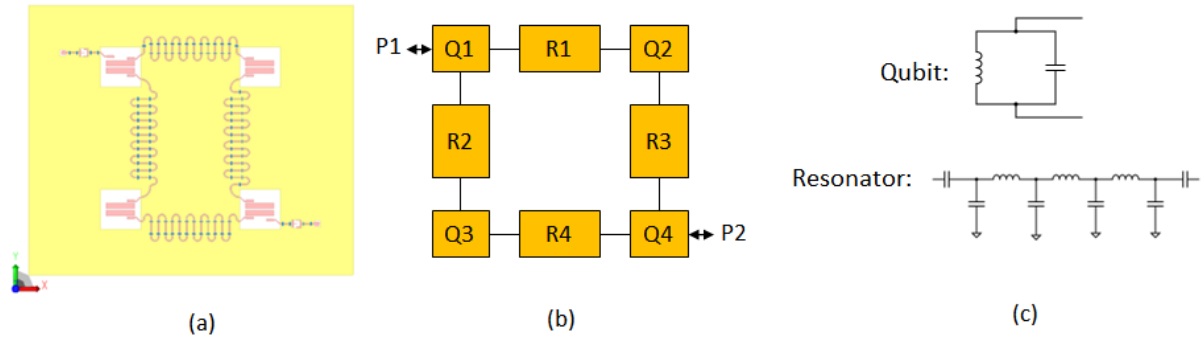

Figure 3. (a) A superconducting circuit layout consisting of four transmon qubits and four meander line resonators. (b) A simple lumped element representation of the superconducting circuit. The Q's are the qubits and the R's are the meander line resonators. (c) The linear circuit representation for the qubit and the meander line resonator.

The superconducting circuit in Figure 3 can be represented as a large network of LC circuits. Note that conductance or resistance is not considered here due to the negligible loss of superconductors. Just as in any LC circuit, resonance is defined as when the reactance of the circuit approaches zero. This is equivalent to when the imaginary part of the admittance across the qubit approaches zero. For example, for Q1, the resonance conditions can be found by finding the frequency where $f_{P1'}(\omega)$ becomes zero [2]. Here, we have

$$f_{P1'}(\omega) = \Im[Y_{P1'P1'}(\omega)] - \frac{1}{\omega L_{j,q1}} + \omega C_{j,q1} \tag{1}$$

$Y_{P1'P1'}(\omega)$ is the admittance seen at the qubit port P1' in the absence of the qubit capacitance and inductance, which can be derived from the scattering parameters at the port. $L_{j,q1}$ and $C_{j,q1}$ are the corresponding qubit inductance and capacitance, respectively. Therefore, the last two terms describe the qubit equivalent circuit. For the qubit n in the network, this equation becomes:

$$f_{Pn'}(\omega) = \Im[Y_{Pn'Pn'}(\omega)] - \frac{1}{\omega L_{j,qn}} + \omega C_{j,qn}$$

Note that $f_{Pn'}(\omega)$ has multiple zeros. One for the qubit (ω_q) and others for each coupled resonator (ω_r') coupled to the qubit. On the other hand, the function $\Im[Y_{Pn'Pn'}(\omega)]$ crosses zeros at a frequency ω_r slightly different from ω_r'. For the circuit in Figure 3, $\Im[Y_{Pn'Pn'}(\omega)]$ crosses zeros twice only for the two coupled resonators. Moreover, since $Y_{Pn'Pn'}$ does not include the qubit, it does not approach zero near the qubit resonance.

Figure 4 shows an example of $\Im[Y_{Pn'Pn'}\ ]$ and $f_{Pn'}(\omega)$ in blue, and orange curves, respectively. The blue curve shows the frequency response of a resonator in the absence of the qubit while the orange curve is the frequency response in the presence of the qubit. There is a slight frequency shift where these curves cross zero: ω_r is the classical resonant frequency of the resonator (high power regime), and ω_r' is the dressed resonant frequency after including the qubit lumped effect (low power quantum regime).

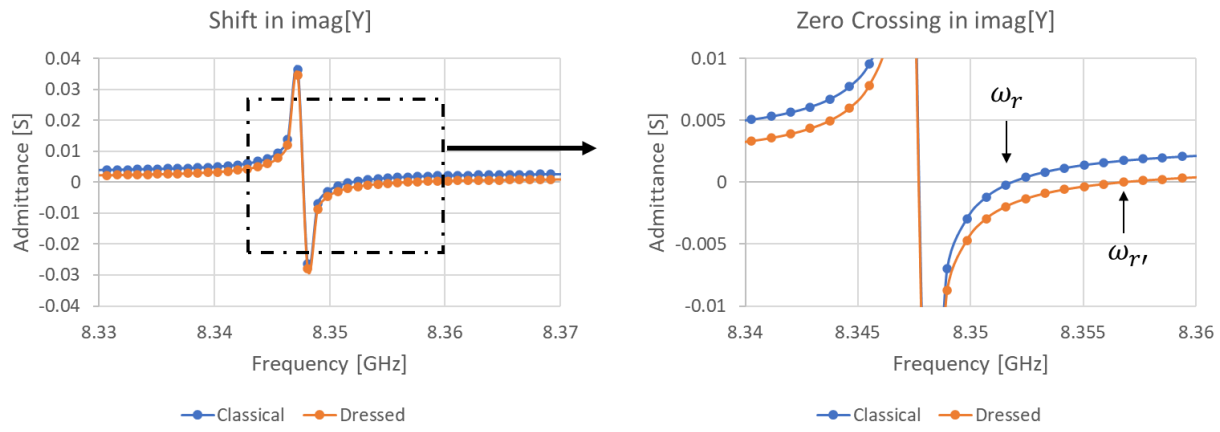

Figure 4. The admittance across the qubit when the qubit is disabled (classical-blue) and when the qubit is enabled (dressed-orange). The resonant frequency changes from ω_r to ω_r' upon including the qubit lumped effect on the circuit.

In circuit quantum electrodynamic (cQED), the dispersive regime describes a condition where the detuning, Δ, or the frequency difference between the qubit and the resonator, is far greater than the qubit-resonator coupling strength, g. In this case, the shift in the resonant frequency, $\omega_r' - \omega_r$, is also known as a dispersive shift:

$$D.S. = \frac{g^2}{\Delta} \tag{2}$$

In experiments, the two distinct transmission spectra can be obtained by changing the excitation power of the circuit using a network analyzer (PNA-X) in initial continuous wave measurements. More details about cQED can be found in Ref. [1, 3, 6].

Next, the anharmonicities of qubits can be calculated from the qubit capacitance just like the quasi-static approach. As discussed earlier, the qubit anharmonicity is $\alpha_q = -E_C = -e^2/2C$. The capacitance (C) for the qubit is obtained from evaluating the qubit port impedance at the resonant frequency. Lastly, the cross-Kerr between a resonator and a qubit can be expressed as:

$$\chi_{qr} = 2\sqrt{\alpha_q \alpha_r} \tag{3}$$

Here, $\alpha_r = -\frac{1}{2}\frac{L_r}{L_J}\frac{C_J}{C_r}E_C$ is the anharmonicity of the resonator, where L_r and C_r are the inductance and the capacitance of the resonator, respectively. The capacitance of the resonator coupled to the qubit is:

$$C_r = \frac{1}{2}f'_{pn}(\omega_r) \tag{4}$$

In Eqn. (4), the prime notation means a derivative with respect to the angular frequency ω. Given the resonant condition for an LC oscillator, the inductance of the resonator can be calculated as follows:

$$\omega_r = \frac{1}{\sqrt{L_r C_r}} \rightarrow L_r = \frac{1}{\omega_r^2 C_r} \tag{5}$$

Note that as Eqn (4) suggests, the resonator capacitance, inductance, and anharmonicity, are effective values seen by one qubit and may differ when calculated using another qubit. For instance, in the circuit from Figure 3, the capacitance, the inductance, and the anharmonicity of R2 may have slightly different values when calculated across the qubit port P1' as opposed to across P3'.

In short, the Full EM Analysis first searches for the resonant frequencies of the qubits and the resonators. Using the capacitance across the qubits, QuantumPro then calculates qubit and resonator anharmonicities. Finally, QuantumPro produces the cross-Kerr between the qubit and resonator modes using Eqn (3). The limitation for the frequency domain method is that it may only return the cross-Kerr strengths between the modes of two elements that are coupled immediately next to one another. This is different from the eigenmode analysis approach, which can calculate the cross-Kerr strengths between any two modes.

Energy Participation Analysis

Next, we explain how the quantum parameters are extracted in the Energy Participation Analysis in QuantumPro. For this analysis, QuantumPro utilizes the eigenmode solver to compute the eigenfrequencies and field patterns to obtain the quantum parameters. This method involves the energy participation ratio (EPR), which represents the fraction of energy of mode m stored in qubit j [4]. QuantumPro first finds distinct modes supported by the qubits and resonators. Then, it computes energy storage across the qubits and resonators when a mode is excited. The latter step requires the energy and voltage integrations for each resonant mode.

The inductive (E_{ind}) and capacitive (E_{cap}) energies of any system are always equal. In a traditional circuit, the former equals the magnetic energy (E_{mag}) stored in the circuit while the latter equals the electric energy (E_{elec}). However, due to the tunneling effect at the qubit junction, we need to include the kinetic inductance energy (E_{kin}). Therefore, the inductive energy becomes:

$$E_{ind} = E_{cap} = E_{elec} = E_{mag} + E_{kin} \tag{6}$$

Then the EPR in a single mode is defined as:

$$EPR = \frac{E_{kin}}{E_{ind}} = \frac{E_{elec} - E_{mag}}{E_{elec}} \tag{7}$$

In a classical cavity geometry, where the electric and magnetic energy quantities are equal, this ratio vanishes. It is also important to note that EPR is denoted as $p_{m,j}$ where m is the mode number and j refers to the qubit. In order to evaluate the EPR in a simple circuit simulation, QuantumPro performs volume integration of electric/magnetic fields of the mode to obtain Eqn. (7). This energy integration approach is straightforward in the case of a single qubit. For multiple qubit cases, calculating the qubit junction current is needed to find the contribution of each junction.

The eigenmodes for a resonator and a qubit are shown in Figure 5. On the left side, it shows the current distribution across a resonator when the resonator mode is excited. On the right side of the figure, there is a strong current across the qubit junction at its resonant frequency. More details about the EPR method can be found in Ref. [4].

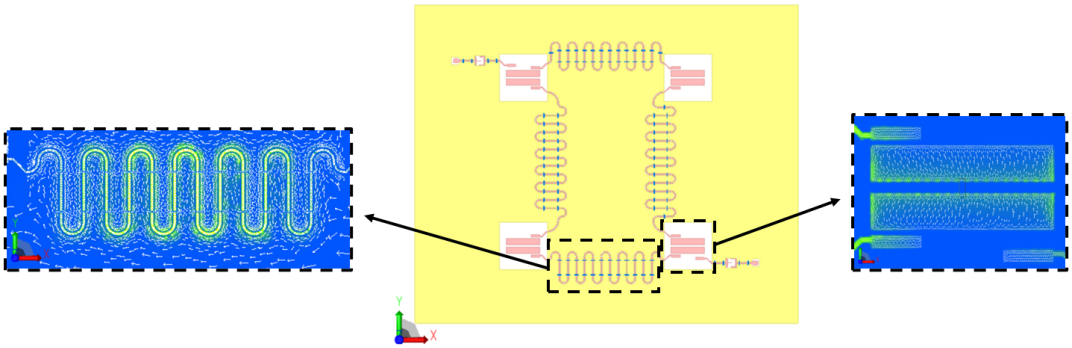

Figure 5. The eigenmode solver finds resonant modes for the qubits and resonators. QuantumPro plots electric/magnetic fields and currents, which can be integrated for quantum parameter calculation.

Since the circuit in Figure 5 has four transmon qubits and four bus line resonators, the circuit supports at least eight eigenmodes and have at least 4 × 8 EPR values; 4 because there are four qubits and 8 because there are eight eigenmodes. For instance, $p_{0,1}$ describes the fraction of the kinetic energy of Qubit 1 to the inductive energy of mode 0. If Qubit 1 is resonant with the mode 0, $p_{0,1}$ would approach unity. If Qubit 1 is not resonant with mode 0, then, $p_{0,1}$ would become much smaller than one.

For multiple qubit circuits, the EPR can be calculated from the energy stored in the junction:

$$p_{mj} = \frac{1}{2} L_j I_{m,j}^2 / E_{ind} \tag{8}$$

Here, L_j is the junction inductance and $I_{m,j}$ is the junction current when the mode is excited. This equation allows for finding the EPR of a qubit for the cross-Kerr calculation. In order to find the junction current when the mode m is excited, QuantumPro first performs path integration of the electric field along the junction path to get the voltage drop across the junction. Figure 6 shows the integration path across the junction. The current across the junction inductance is then the voltage drop divided by the junction's inductive impedance ($j\omega L_j$).

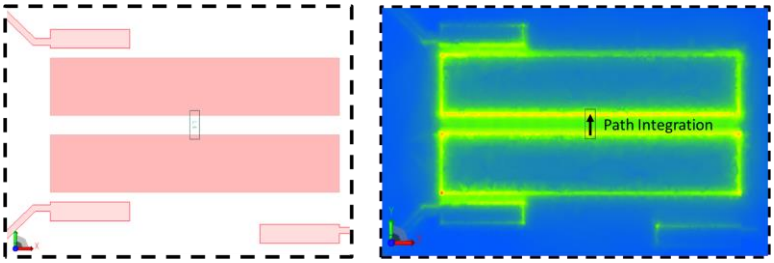

Figure 6. The path integration of the electric field along the junction (shown as a black arrow) yields the voltage drop across the junction.

Next, we discuss the Kerr matrix (χ), which is a square matrix containing the anharmonicities and cross-Kerr strengths. The diagonal elements of the matrix, when $m = n$, represent the anharmonicities of the qubits and resonators and the off-diagonal elements, $\chi_{mn} = \chi_{nm}$ represent cross-Kerr strengths, which relate to the coupling between qubits and resonators. The elements of the cross-Kerr elements in the matrix are defined in the general form:

$$\chi_{mn} = \sum_{j=1}^{J} \frac{\hbar \omega_m \omega_n}{4E_j} p_{mj} p_{nj} \tag{9}$$

Here, *m* and *n* are two modes of the superconducting circuit and j refers to qubits. $\omega_{m/n}$ is the angular frequency for the mode *m* or *n such that* $m \neq n$. E_j is the junction energy for the qubit:

$$E_j = \frac{\Phi_0 I_{c,j}}{2\pi} \tag{10}$$

Φ_0 is the magnetic flux quantum, or $h/2e$. $I_{c,j}$ is the critical current of the qubit. Using the relation $L_j = \Phi_0/(2\pi I_C)$, where L_j is the junction inductance, the junction energy can be expressed as $E_j = \Phi_0^2/(4\pi^2 L_j)$. The cross-Kerr representing one qubit mode and one resonator mode relates to the shift of the resonator frequency due to the coupling effect of the qubit.

Lastly, the diagonal elements in the matrix represent the anharmonicity ($\alpha_{q/r}$) of a qubit or a resonator as follows:

$$\chi_{mm} = \alpha_{q/r} \tag{11}$$

From this relation, the anharmonicity can be defined as:

$$\alpha_{q/r} = \sum_{j=1}^{J} \frac{\hbar\omega_m^2}{8E_j} p_{mj}^2 \tag{12}$$

Given the total N eigenmodes, the χ matrix becomes an N-by-N square matrix. It is worth noting that the eigenmode analysis allows for calculating any combinations of cross-Kerr strengths between any two modes. For instance, the cross-Kerr strength between two qubits or two resonators that are not directly connected is non-zero albeit small. This value cannot be directly extracted in the frequency domain analysis.

One Qubit One Readout Resonator Model

In this section, we use the PathWave ADS Quantum example of a basic circuit consisting of a single qubit and a single readout resonator, as shown in Figure 7. We run the Full EM Analysis with the MoM solvers in QuantumPro for the quasi-static (QS) method using Momentum RF and the frequency domain (FD) method using Momentum Microwave. We then run the Energy Participation Analysis (EPR) with the FEM eigenmode solver and compare the anharmonicities and the cross-Kerr strength of the qubit and the resonator calculated from the three solvers. For this example, we set the frequency range from 4 GHz to 10 GHz since the qubit and resonator mode frequencies all lie within this range.

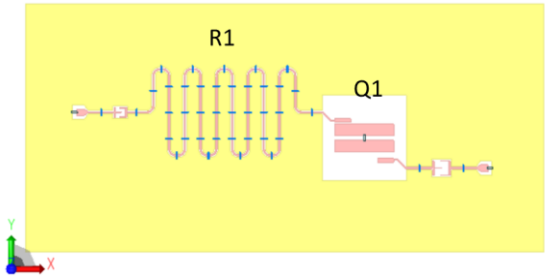

	Momentum RF	Momentum Microwave	Eigenmode Solver
Q1	6.12 GHz	6.12 GHz	5.98 GHz
R1	8.36 GHz	8.36 GHz	8.14 GHz

Figure 7. One qubit and one readout resonator example. The qubit has an inductance of 11 nH. The table on the right shows the resonant frequencies for the qubit and the resonator solved using three different solvers.

In order to obtain accurate results, we first refine the mesh densities. For all momentum simulations, users may first set the general mesh density and refine the meshing around the qubits. For instance, in the Momentum RF and Momentum Microwave simulations, we set the general mesh 200 cells per wavelength (cpw). This means within one wavelength distance corresponding to the highest frequency, QuantumPro enforces 200 meshing cells. In addition, the mesh points near the qubit port also need to be refined. We pick 2000 cpw so that it ensures that the geometry has more mesh points near the qubit junction for an accurate analysis of the capacitive effects.

For the Energy Participation Analysis in QuantumPro, users should refine the mesh parameters on the central conductor of the coplanar waveguide. For this example, we set the meshing finer (~ 5 µm) on the center conductors of the meander lines and the charge islands of the qubit while leaving the mesh points at normal density on the ground planes and on the air bridges. The resulting mesh plots for the Momentum RF/Microwave and the FEM eigenmode solver are shown in Figure 8.

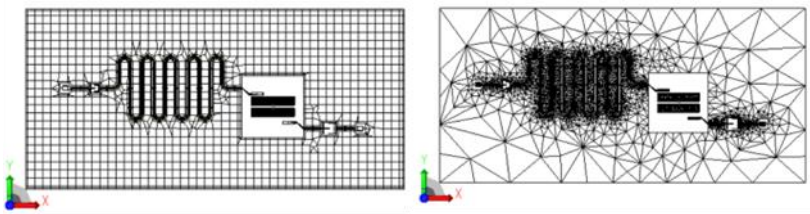

Figure 8. The mesh plots for the one qubit and one readout example for (a) QuantumPro Momentum RF/Microwave and (b) QuantumPro FEM Eigenmode Solver.

We set the qubit (Q1) junction inductance as 11 nH and neglect the junction capacitance. The junction capacitance will slightly influence the eigenfrequency of the qubit and it can be easily incorporated in the lumped component model if needed. Once the simulation is finished, QuantumPro utilizes Eqn (1) to calculate the mode frequencies of the qubit and the resonator for the MoM solvers. For the FEM eigenmode solver, the main solutions are the mode frequencies and the corresponding quality factors. In both cases, QuantumPro extracts and displays the χ matrix in a tabular form, as shown in Figure 9. Given the mesh parameters are properly set, both analyses should yield resonant frequencies that agree reasonably well with one another.

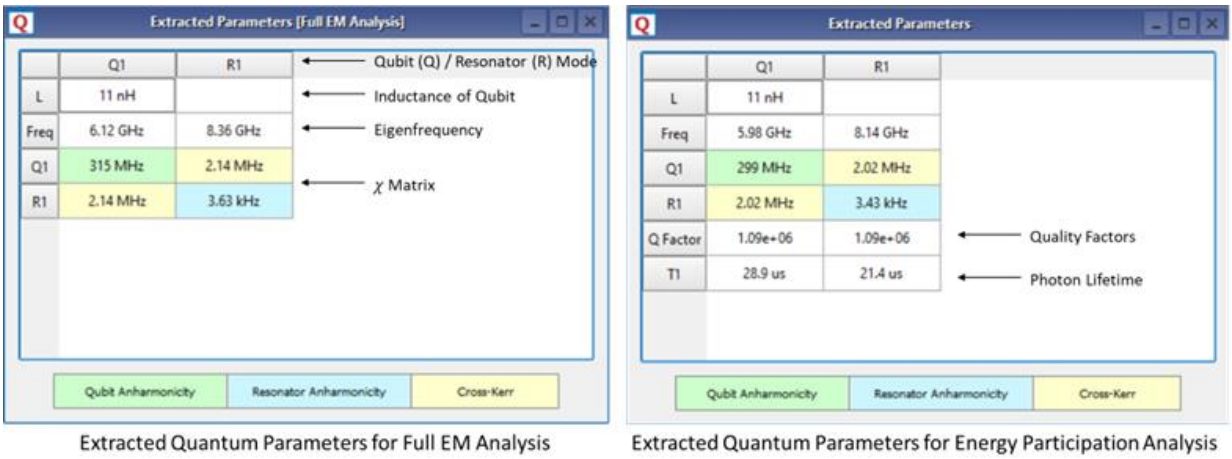

Figure 9. QuantumPro extracts and displays the χ matrix in a tabular form. The colored cells represent the χ matrix elements. The Energy Participation Analysis (right) reports the quality factors and the photon lifetimes (T1) of the qubit and resonator modes in addition to the χ matrix and the eigenfrequencies.

Table 1 shows the anharmonicity of the qubit extracted by QuantumPro using the different solvers. The results from the Full EM Analysis quasi-static (QS-Momentum RF) and frequency domain (FD-Momentum Microwave) simulators are almost identical. The Energy Participation Analysis (EPR) yielded an anharmonicity that agrees well with the results of the other two methods (within 5%). It's important to emphasize that meshing holds a crucial role in determining the precision of the different techniques. Typically, enhancing the mesh would result in an improved alignment, albeit with an increase in computational time. In this context, we're striking a balance between maintaining acceptable accuracy and avoiding excessive computational expenses.

Table 1. The anharmonicity of the qubit extracted from three different analyses. The results show good agreement among the Full EM Analysis Quasi-static (QS-Momentum RF), the Frequency Domain (FD-Momentum Microwave), and the Energy Participation Analysis (EPR).

	C (QS)	C (FD)	α (QS)	α (FD)	α (EPR)
Q1	61.53 fF	61.53 fF	314.82 MHz	314.84 MHz	298.80 MHz

In addition, Table 2 compares the cross-Kerr strengths for the one qubit one resonator example using the different methods. The cross-Kerr strengths agree well between the Full EM Analysis (QS and FD) and the Energy Participation Analysis (EPR). In general, the EPR with a refined meshing strategy typically yields the most accurate results. The resonator anharmonicity is also listed in Table 2.

Table 2. The cross-Kerr and the resonator anharmonicity for the one qubit one resonator example.

χ_{Q1R1} (QS)	χ_{Q1R1} (FD)	χ_{Q1R1} (EPR)	α_{R1} (QS)	α_{R1} (FD)	α_{R1} (EPR)
2.14 MHz	2.14 MHz	2.02 MHz	3.62 kHz	3.63 kHz	3.43 kHz

To summarize, the quantum parameter extraction of a basic one qubit one resonator quantum circuit was presented in this section. The Full EM (quasi-static and frequency domain methods) and the Energy Participation Analyses yielded qubit anharmonicities in good agreement. Similarly, a strong alignment was observed in the cross-Kerr strength calculated through the different methods. In the next section, we focus on a more complex example with multiple qubits and resonators.

Four Qubits Four Resonators Model

We present another study to compare the quantum parameters for a more complex circuit. The example, here, consists of four qubits and four resonators, as shown in Figure 10. This circuit is another design flow example of PathWave ADS. Just like the previous example, we use the Full EM Analysis and the Energy Participation Analyses to calculate the anharmonicities and the cross-Kerr strengths of qubits and resonators using the quasi-static (QS) Momentum RF, frequency domain (FD) Momentum Microwave, and the FEM eigenmode solvers.

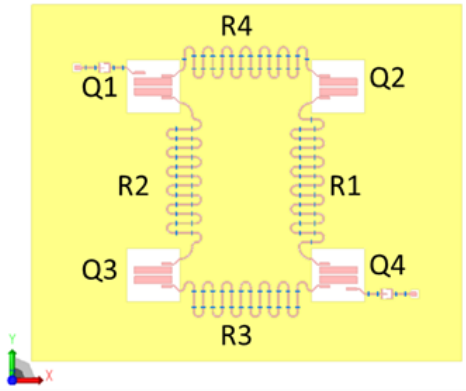

	QS	FD	EPR
Q1	5.95 GHz	5.95 GHz	5.76 GHz
Q2	6.10 GHz	6.10 GHz	5.87 GHz
Q3	6.30 GHz	6.30 GHz	5.98 GHz
Q4	6.44 GHz	6.44 GHz	6.13 GHz
R1	8.65 GHz	8.65 GHz	8.31 GHz
R2	8.92 GHz	8.92 GHz	8.55 GHz
R3	9.41 GHz	9.41 GHz	9.01 GHz
R4	9.67 GHz	9.67 GHz	9.29 GHz

Figure 10. The qubits and resonators. The inductances for the qubits are 11.5 nH, 11.0 nH, 10.5 nH, and 10.0 nH for Q1, Q2, Q3, and Q4, respectively. Among the resonators, R4 supports the highest eigenfrequency mode while R1 supports the lowest eigenfrequency mode.

For accurate results, we take careful steps to refine the meshes for the circuit. The resulting mesh plots for Momentum RF (QS), Momentum Microwave (FD), and the FEM eigenmode solver (EPR) are shown in Figure 11. Over the frequency span from 4 GHz to 10 GHz, for the Momentum RF and Momentum Microwave, the general mesh density was set at 100 cpw. We refine meshing near all qubit ports to 1000 cpw. Lastly, for the eigenmode solver, we set the mesh size of the center conductors for the qubits and resonators equal to 5 µm. The necessity to strike a balance between mesh refinement and computational time becomes even more significant when dealing with circuits with a larger number of qubits.

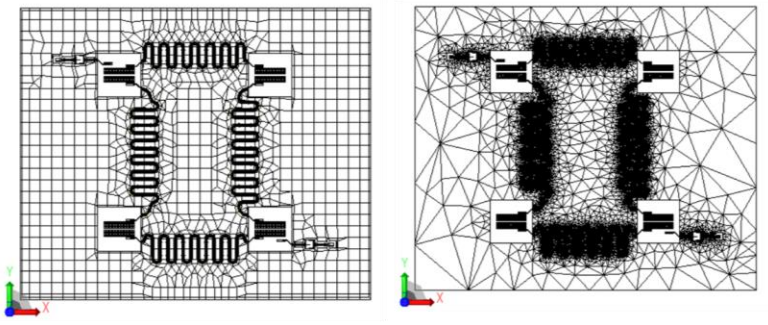

Figure 11. The mesh plots for the four qubits and four resonators example for (a) QuantumPro Full EM Analysis (Momentum RF/Microwave solvers) and (b) QuantumPro Energy Participation Analysis (FEM Eigenmode solver).

The four qubits are designated as Q1, Q2, Q3, and Q4 with the inductances 11.5 nH, 11.0 nH, 10.5 nH, and 10.0 nH, respectively, as shown in Figure 10. In this context, we neglect the junction capacitance, as its impact is minor when compared to the capacitance originating from the surrounding environment. The qubits in this geometry yield four distinct eigenfrequencies, with Q4 having the highest resonant mode and Q1 the lowest, as listed in Figure 10. The resonant frequencies from the Full EM Analysis (QS-Momentum RF, and FD-Momentum Microwave) and the Energy Participation Analysis (EPR-FEM eigenmode) differ by about 5% or less for all qubits and resonators. The Full EM Analysis results tend to have a higher resonant frequency than the results from the Energy Participation Analysis. This is expected as the Method of Moments (MoM) generally underestimates the capacitive effect of electromagnetic circuits. We lessen this by fine-meshing the islands of the transmons.

The anharmonicity calculations for the three different methods are shown in Table 3. The capacitance calculations for the quasi-static method (QS-Momentum RF) and the frequency domain method (FD-Momentum Microwave) in the Full EM Analysis were almost identical. The difference in qubit anharmonicity between the frequency domain analysis and the eigenmode analysis is around 10%. Further refinement of the mesh settings would lead to more concordant results but at a higher computational cost.

Table 3. Excellent agreement for qubit capacitance between the Quasi-static (QS-MoM RF) and the Frequency Domain (FD-MoM Microwave) Analysis. The anharmonicities from the Energy Participation Ratio (EPR) calculation deviate slightly from QS and FD.

	C (QS)	C (FD)	α (QS)	α (FD)	α (EPR)
Q1	62.25 fF	62.24 fF	311.20 MHz	311.21 MHz	287.62 MHz
Q2	61.98 fF	61.97 fF	312.55 MHz	312.56 MHz	286.26 MHz
Q3	60.81 fF	60.81 fF	318.53 MHz	318.54 MHz	283.20 MHz
Q4	61.13 fF	61.12 fF	316.90 MHz	316.91 MHz	282.39 MHz

Furthermore, we compare the cross-Kerr strengths obtained from different methods in Table 4. While the Full EM Analysis allows for computing the quantum parameters for only the two modes supported by qubits/resonators that are connected and coupled, the Energy Participation Analysis allows for calculating cross-Kerr values between any two modes. The difference in the cross-Kerr strengths is about 15%. The accuracy of the different techniques can be improved by making the mesh points finer at the cost of computational time. Again, the EPR with a refined meshing strategy typically yields the most accurate results.

Table 4. The cross-Kerr strengths between qubits and resonators from the Full EM Analysis (QS-MoM RF and FD-MoM Microwave) and Energy Participation Analysis (EPR-FEM eigenmode).

	χ_{QR} (QS)	χ_{QR} (FD)	χ_{QR} (EPR)
χ_{Q1R2}	1.70 MHz	1.71 MHz	1.62 MHz
χ_{Q1R4}	1.22 MHz	1.23 MHz	1.09 MHz
χ_{Q2R1}	2.06 MHz	2.07 MHz	1.87 MHz
χ_{Q2R4}	1.42 MHz	1.43 MHz	1.23 MHz
χ_{Q3R2}	2.26 MHz	2.27 MHz	1.82 MHz
χ_{Q3R3}	1.69 MHz	1.70 MHz	1.39 MHz
χ_{Q4R1}	2.97 MHz	2.99 MHz	2.42 MHz
χ_{Q4R3}	1.80 MHz	1.80 MHz	1.51 MHz

Not listed in Table 4 are the cross-Kerr strengths between non-adjacent elements available from the Energy Participation Analysis (refer to Eqn. (9)). For instance, Q1 and R3 are not directly adjacent to one another. It is not possible to find the cross-Kerr between these two elements in the Full EM Analysis. This minute value is about 1.2 kHz, which can be calculated using the Energy Participation Analysis.

Lastly, Table 5 shows the anharmonicities of the resonators using the three different solvers. The Full EM Analysis (QS-MoM RF and FD-MoM Microwave) yields two anharmonicity values for each resonator (looking from the two individual qubits to which each resonator is linked to, as shown in Figure 10). The resonator anharmonicities in Table 5 for QS and FD report the average of the two values.

Table 5. The anharmonicities of the resonators

	α_{RR} (QS)	α_{RR} (FD)	α_{RR} (EPR)
R1	10.4 kHz	10.5 kHz	8.2 kHz
R2	6.32 kHz	6.41 kHz	5.21 kHz
R3	4.79 kHz	4.82 kHz	3.72 kHz
R4	2.80 kHz	2.86 kHz	2.35 kHz

Figure 12 depicts the results of quantum parameter extraction for the four-qubit-four-resonator example using the Full EM Analysis and the Energy Participation Analyses. The qubit anharmonicity are in good agreement, while the cross-Kerr calculations had a varying degree of discrepancies but had a reasonable consensus. We expect to get accurate quantum parameters when we apply these methods to even more complex circuits. However, as the circuits become larger and more complicated, the computational time would also grow, and a more sophisticated meshing scheme may help to obtain accurate results while conserving computational resources. Furthermore, the EM high performance cloud (HPC) accelerator of PathWave can be leveraged to enable parallel EM simulation to speed up the analysis for the frequency domain analysis.

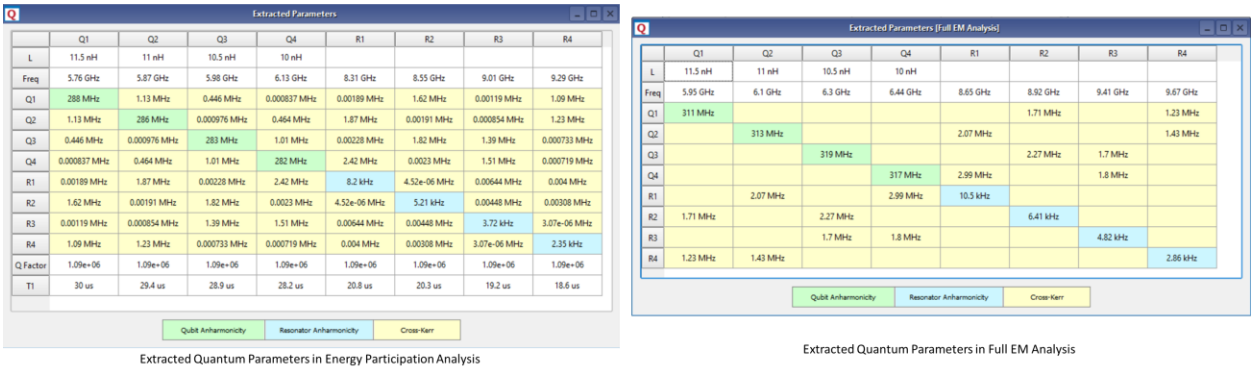

Figure 12. QuantumPro extracts and displays the χ matrix is a tabular form. The colored cells represent the χ matrix elements. While the Energy Participation Analysis (left) produces a full matrix with non-zero elements for all off-diagonal elements, the Full EM Analysis (right) have only the cells that reflect coupling between the neighboring elements.

Conclusion

QuantumPro allows for modeling superconducting qubit circuits, analyzing their EM performance and their nonlinear properties in the quantum regime with ultra-low power signal excitation. The Full EM Analysis supports frequency sweep of the circuits using the MoM and FEM solvers. From the scattering parameters, QuantumPro calculates the resonant frequencies and the quantum parameters. Additionally, the Energy Participation Analysis supports the FEM Eigenmode solver, which calculates the eigenfrequencies of the qubits and the resonators. From the energy participation ratios, QuantumPro calculates the quantum parameters.

In this application note, we described the methods that QuantumPro utilizes to extract quantum parameters. We showed two QuantumPro models, the one-qubit-one-resonator and the four-qubit-four-resonator examples. Employing Momentum RF, Momentum Microwave, and FEM Eigenmode solvers, we derived and compared the quantum parameters that were in reasonable agreement. The MoM solvers require less computational resources compared to the FEM solvers due to the fewer number of unknowns. On the other hand, the FEM Eigenmode solver allows for finding a full χ matrix while the frequency domain solvers yield the entries in the χ matrix that only represent the interactions between neighboring elements.

References

1. Krantz et al. "A quantum engineer's guide to superconducting qubits." Applied physics reviews 6.2 (2019): 021318.
2. Nigg et al. "Black-box superconducting circuit quantization." Physical Review Letters 108.24 (2012): 240502.
3. Dassonneville et al. "Fast high-fidelity quantum nondemolition qubit readout via a nonperturbative cross-Kerr coupling." Physical Review X 10.1 (2020): 011045.
4. Minev et al. "Energy-participation quantization of Josephson circuits." npj Quantum Information 7.1 (2021): 131.
5. Minev et al. "Circuit quantum electrodynamics (cQED) with modular quasi-lumped models." arXiv preprint arXiv:2103.10344 (2021).
6. Blais et al. "Cavity quantum electrodynamics for superconducting electrical circuits: An architecture for quantum computation." Physical Review A 69.6 (2004): 062320.
7. Koch et al. "Charge-insensitive qubit design derived from the Cooper pair box." Physical Review A 76.4 (2007): 042319.

Keysight enables innovators to push the boundaries of engineering by quickly solving design, emulation, and test challenges to create the best product experiences. Start your innovation journey at www.keysight.com.

KEYSIGHT

This information is subject to change without notice. © Keysight Technologies, 2023, Published in USA, August 30, 2023, 3123-1662.EN